Draft version August 18, 2015
Preprint typeset using LaTeX style emulateapj v. 12/16/11

VARIABILITY OF PLANETARY MASS COMPANION 2M1207 B

Yifan Zhou, Daniel Apai, Glenn Schneider, ...
The University of Arizona
Draft version August 18, 2015

ABSTRACT

...
Subject headings: kw1, kw2, ...

1. INTROCDUCTION

2. OBSERVATION

We took high contrast direct imaging observation of 2M1207 system on UT 2014 April 11 using HST. (*HST* Proposal GO-13418, PI: D. Apai). The data were acquired with the Wide Field Camera 3 (WFC3) in filter F125W ($\lambda_{\rm pivot}$ = 1245.9 nm, full width at half maximum (FWHM) = 301.5 nm) and F160W ($\lambda_{\rm pivot}$ 1540.52, FWHM = 287.9 nm) using the 256×256 sub-array mode. We observed 2M1207 system in six contiguous HST orbits and obtained a data-set that have a temporal resolution of $\sim$ 1.5 minutes and baseline of 8 hours and 40 minutes, interrupted by Earth occultaions of 58 minutes every 94 minutes.

The observations was initially designed to apply two-roll point spread function (PSF) subtraction (e.g. Song et al. (2006)) to remove the background light from the primary star. The telescope roll angles for data taken in orbit 1, 3, 5 and those taken in orbit 2, 4, 6 differed by 25°, thus the roll displacement of the companion is 0.34″ that is 2.75 and 2.30 resolution elements in F125W and F160W respectively. In each orbit we took a sequence of 13 SPARS10 exposures with NSAMP=10, alternating between F160W and F125W filters, with 2-3 identical exposures in one exposure sequence. To improve PSF sampling and reduce the risk caused by bad pixels, we applied standard 4 point dithering. In each orbit, exposures were taken with dithering position 1 – 4 sequently. Over the 6 orbits, we obtained 70 multi-acuum images for filter F125W and 64 images for filter F160W with exposure time of 88.4 seconds for both two filters.

3. DATA REDUCTION

Through the whole analysis, we used the `flt` files that were produced by WFC3's `calwfc3` pipeline. The `flt` files were reduced with calibration steps including dark current correction, non-linearity correction, and flat field correction. A further step of up-the-ramp fit was applied to combine all non-destructive reads and remove cosmic rays. Although Mandell et al. (2013) stated that WFC3 IR time series extract from `flt` files have a rms 1.3 times larger than that obtained from `ima` files , `flt` files keeps all pixels of the image of 2M1207 A unsaturated, while in 80% of non-destructive reads the cores of 2M1207 A are saturated. Thus `flt` files help better align the images for primary subtraction, and separate the flux of 2M1207 B from that of 2M1207A.

The small angular separation of 2M1207 A and B (as shown in Figure 1) makes precise primary star subtraction and photometry very difficult. On the under-sampled WFC3 IR detector (plate scale $\sim 0.13''$pixel^{-1} Dressel (2012)), the primary and the secondary only separate by $\sim$ 6 pixels, which is about 5 times of the FWHM of the PSF. In addition, under-sampling causes significant artifacts when shifting the images for registration no matter what interpolation method is used.

3.1. *Tiny Tim PSF Photometry*

To over come the difficulty, we make use of the Tiny Tim PSF simulator to pursue high precision photometry under this extreme circumstance. Tiny Tim can produce model PSF based on the filter, spectrum of target, focus status, and the telescope jitter. One significant advantage of Tiny Tim PSF over empirical PSF is that Tiny Tim can produce Nyquist sampled PSF, which makes image shifting and interpolation rather straight forward. One essential disadvantage of Tiny Tim is that the model PSFs have significant systematic errors. Biretta (2014) demonstrated that the diffraction spikes and coma are not well simulated with Tiny Tim for WFC3 IR images. However, using the 6-orbit long time series, we are able to well characterize the difference of model PSFs and empirical PSFs. By modeling the difference and combining it with model PSFs, we can produce high quality hybrid PSFs to significantly improve the PSF simulation and PSF photometry.

We started the reduction by making bad pixel masks for every image. Pixels with data quality flags "bad detector pixels" (DQ = 4), "unstable response" (DQ = 32), and "bad or uncertain flat value" (DQ = 512) were masked out and excluded from further analysis as suggested by previous transit exoplanet spectroscopic observations(e.g. Berta et al. 2012; Kreidberg et al. 2014).

We then produced a list of 10x over-sampled PSFs based on the positions and spectrum (Bonnefoy et al. 2014) of 2M1207 A with different telescope jitter ranging from 0 to 50 mini-arcsec s^{-1} in both x and y directions. We used the new set of Tiny Tim parameters provided by Biretta (2014) to better model the cold mask, diffraction spikes, and the coma. The focus parameters were calculated using the model listed on the STScI website[1]. The PSFs were registered with the original image by searching on a dynamic grid and minimizing the difference of observation and model PSF at a region centered on 2M1207 A with the image of 2M1207 B mostly excluded. The best fitted primary star position and telescope jitter were obtained in this step. Then, we generated the PSF

[1] http://www.stsci.edu/hst/observatory/focus/FocusModel

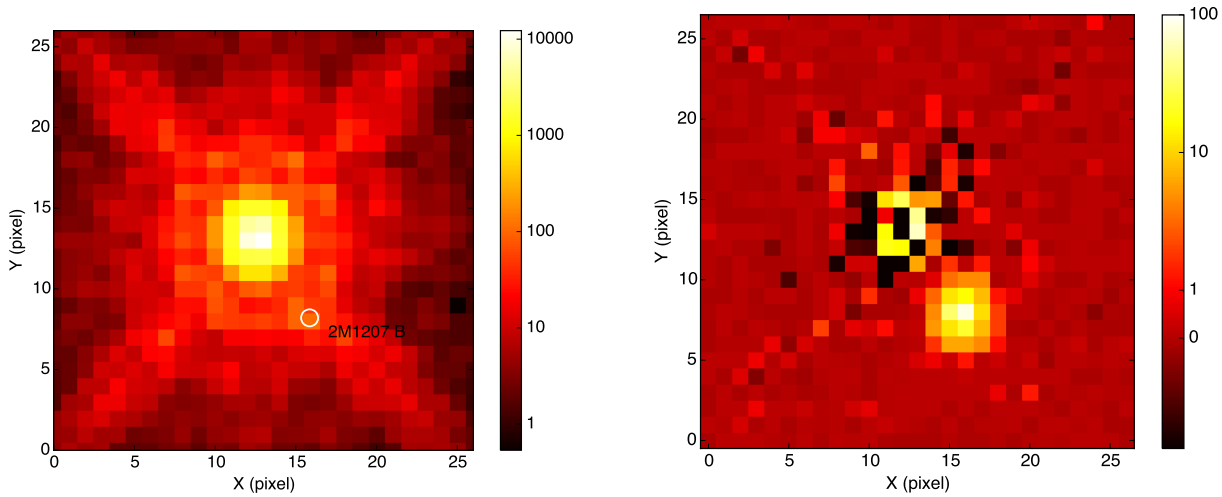

FIG. 1.— WFC3 F160W images of 2M1207A system. Upper: original image, lower: residual model and primary PSF subtracted. The image of 2M1207 B is overshadowed by the halo of the image of 2M1207A and can be hardly seen from the original image. With a hybrid PSF (residual + Tiny Tim PSF) subtraction, the image of 2M1207 B is clearly displayed.

for 2M1207 B based on its position on detector, spectrum (Patience et al. 2010), and the telescope jitter that had been obtained above. In the final step, we combined the two PSFs together. We fixed the position of the primary as it had been fitted in the first step and fitted for the amplitudes of the two PSFs and the precise position of the secondary. Since the total fluxes of the model PSFs were normalized to unity as default, the fluxes of 2M1207 A and B were solely represented by the amplitude of the two PSFs coordinately.

Because of the systematic errors of the Tiny Tim PSF, the quality of the fitting is not optimistic. The reduced χ^2 values were at level of ~ 10. However, we found that the residual patterns were very stable among the image that have the same dithering position and telescope rolling. Therefore, we median combined the residual images that have the same dithering position and telescope rolling angle to construct 8 residual models (4 dithering position $\times$ 2 telescope rolling angle) for each filter. We pre-subtract the corresponding residual from the original image and repeated the procedure that listed above. Using this extra-step, the reduced χ^2 greatly decreased to around unity.

3.2. *Uncertainty analysis*

3.2.1. *White noise*

The difficulties of high contrast photometry is finally exhibited by the error bars of the measurement. The scatterings of the photometric measurements are dominated by photon noise. We estimated the photon noise by calculating the total flux within a 3-pixel (0.39 arcsec) aperture centered on 2M1207 B. The photon noises for F125W and F160W photometry are 2.1% and 1.2%. These calculation results are at the same level of the scattering of the photometric time series.

3.2.2. *Flat field uncertainties*

In our observation, 2M1207 B were taken exposure at 8 different spots on the detector (2 rolls $\times$ 4 dithering positions). The uncertainties in the flat field are potential sources of variation. The uncertainty of WFC3 IR pipeline flat field is $\sim$ 1% (Dressel 2012) and our time resolved observation for another target demonstrate that aperture photometry for exposures taken at different dithering position have scatterings at the same level.

Flat field uncertainties have smaller effects on PSF photometry since multiple pixels are fitted simultaneously. To verify this, we multiplied an artificial flat field error mask that is a uniform distributed Gaussian noise array with mean of 1 and sigma of 1% to every image, and repeat the PSF photometry routine with the error-applied images. We obtained almost same photometry measurements as the original.

However, PSF profile changes with different exposure positions due to pixelation, especially for the case that WFC3 IR is significantly under-sampled. Also, the flat fields may potentially have large scale structures (Dressel 2012). Because of these factors, The fluxes for both 2M1207 A and B are clearly correlated with the dithering position. To reduce the correlation, we normalize each group of exposures that have the same dithering position and roll angle individually – we took the median of the fluxes that were measured from these exposures as normalization factors and devided them from every photometric measurement. Because the normalization factor for each group of exposures is calculated across the whole observation, this normalization step have negligible impacts on variability analysis.

3.2.3. *Validity tests for the variability*

Because the aim of this letter is to search for temporal change, it is essential to exclude the possibility that variability is systematic artifacts.

We fitted sinusoidal waves to both of the F125W and F160W light curves to preliminarily quantify the variability. The periods of the best fitted sine function of the two light curves are similar, 10.9 hour for F125W and 9.3 hour for F160W, and the periods fitted here are not related with any WFC3 instrumental periods. The similarity of the period measurements is a proof that the variability is physical.

Due to image persistence effect, the first orbit of HST observation is often problematic, and is neglected by sev-

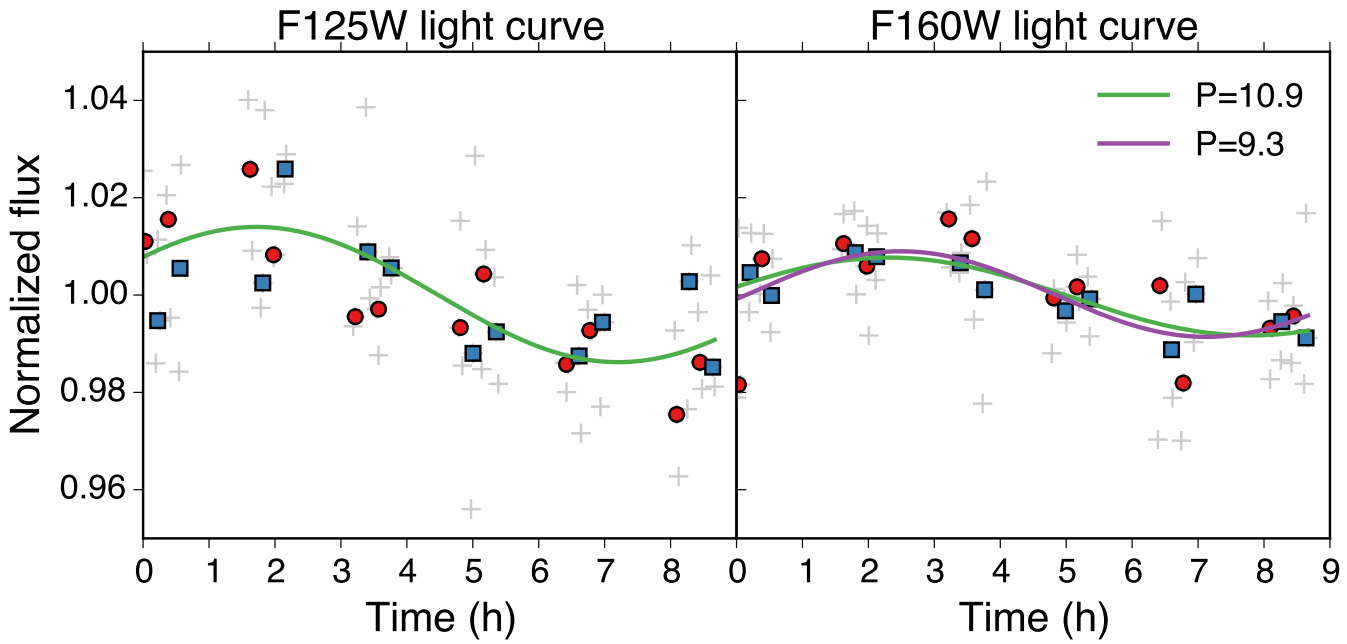

FIG. 2.— Normalized light curves for 2M1207B with filter F125W (left) and F160W (right). Original photometric measurements are plotted with gray crosses. The two halves of data are binned individually, and plotted with red points (first half) and blue squares (second half). The F160W light curves are plotted with two fitted sinusoidal curves, The green curve is fitted with the period fixed to be same as the F125W and the purple curve is fitted with all parameter set free.

eral analyses (**citation?**). In our analysis, the fluxes measured from 2M1207 A are significantly lower in the first lower (Figure 3) than those measured from rest fo the orbits. The exposure levels at the pixels of the peak of the PSF of 2M1207 B are less than 10000 e^- for both two colors, thus image persistence is less of an issue for 2M1207 B. To further exclude this effect, we fitted sinusoidl waves to the light curves without using the first orbit, and obtained similar results.

To rule out the possibility that the variability is introduced by data reduction, e.g., the normalization step, we split the data into two halves – the first half is the data taken at dithering position 1 and 3, and the second half is that for ditheirng position 2 and 4. For each half, we repeat the analysis independently. For both of F125W and F160W, two halves demonstrated similar trend of variability as shown in Figure 2.

4. RESULT

We obtained high signal to noise photometry series for both 2M1207 A and B (Figure 3). On average, the photometric contrast is 6.52 ± 0.03 for F125W and 5.77 ± 0.02 for F160W. The difference of F125W contrast from that measured in J-band (Mohanty et al. 2007) and F160W contrast from that measured with NICMOS F160W (Song et al. 2006) is due to the different throughput profiles of the filters.

Although the photometric time series demonstrate relatively large scattering, both F125W and F160W light curves demonstrate sinusoidal shape with clear temporal variability. We fitted sine waves to the two light curves using least square optimization, and determined the periods and variation amplitudes. The best fitted periods for F125W and F160W are 10.9 and 9.3 hour correspondingly. The amplitudes for the normalized light curves are 1.4% and 0.9% for F125W and F160W light curves.

To constrain the uncertainties of the least square optimization results, we used a Monte Carlo(MC) method to improve the fitting. We generated a series of random Gaussian noises with the standard deviation same as the photon noise, added them to the original light curves, and applied least square fit to the new light curves. We repeated above routine for 10000 times and obtained the distribution of the fitting parameters. The distributions for the periods and the amplitudes for F125W and F160W light curves are shown in Figure 4.

The distributions for the periods demonstrate long tail shaped towards long period. The peaks of the two distributions separated by ~ 1 hour. The difference of the peaks are within $1-\sigma$. Combing the measurements from the two light curves, we conclude the rotation period of 2M1207B to be $9.0^{+2.5}_{-1.5}$ hours.

The variation amplitudes in the two bands have significant difference. The distributions of the amplitudes are well described by Gaussian profiles. To fit the histogram to a Gaussian function, we determined that amplitude distribution of F125W peaks at 1.5% with a standard deviation of 0.3%, and that of F160W have mean and standard deviation of 0.9% and 0.2% correspondingly. The peaks of the two histograms separated by more than $2-\sigma$. The variation amplitude of F125W light curve is 1.67 times of that of F160W light curve.

5. DISCUSSION

- a data-reduction pipeline is developed to obtain high precision photometry measurement from high contrast WFC3 IR data. For a contrast of ~ 7 magnitudes at an angular separation of $\sim 0.7''$, we obtained photometry measurement for 2M1207 B at precision of about 2-3%.

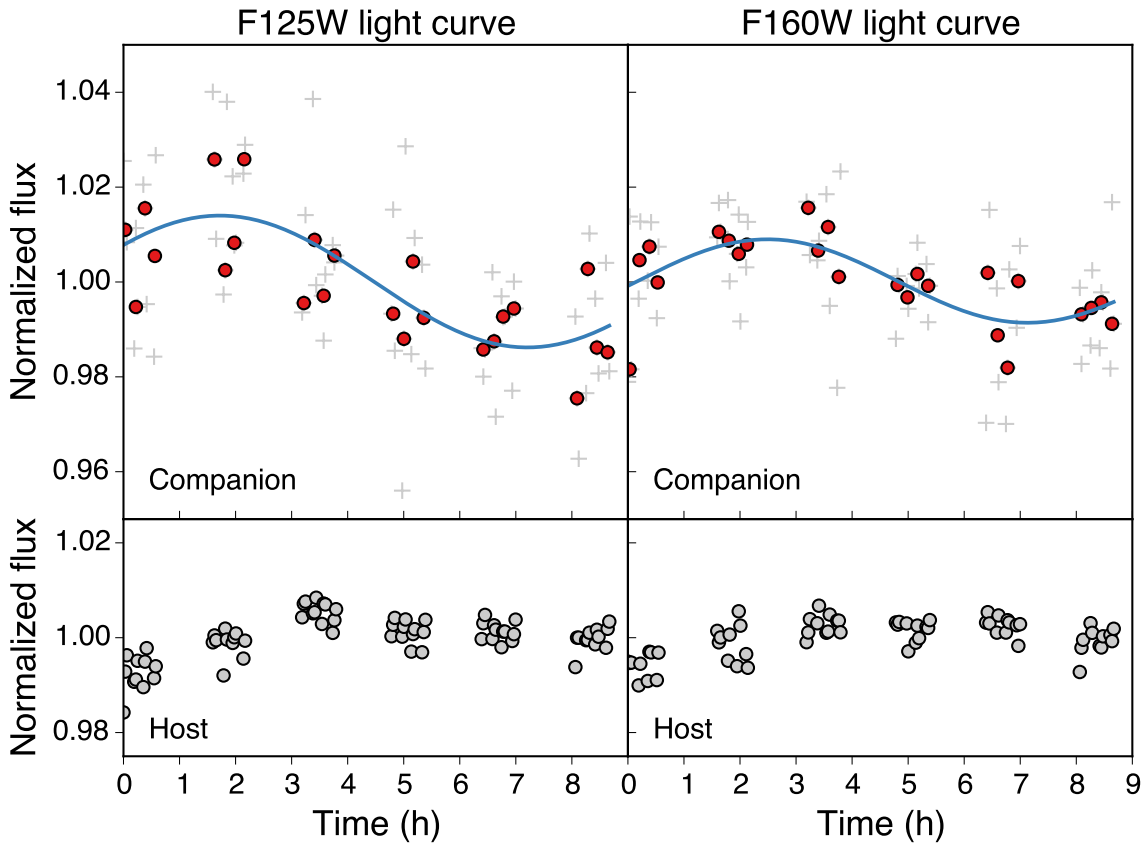

FIG. 3.— Normalized light curves for 2M1207 B (upper) and A (lower) with filter F125W (left) and F160W (right). Individual photometric measurement are plotted in gray crosses and binned photometry are plotted with red points. Best fitted sinusoidal waves are plotted with blue solid lines.

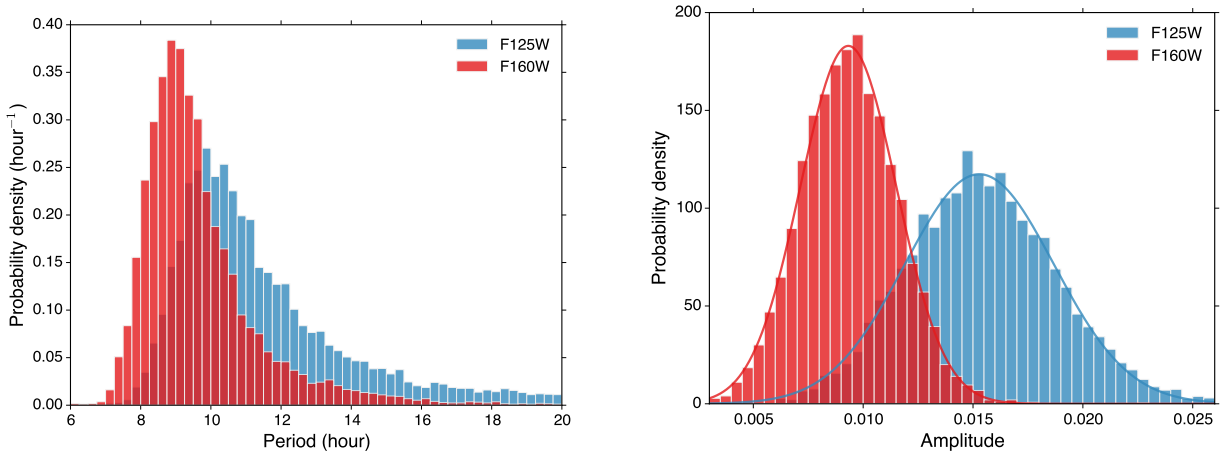

FIG. 4.— Distributions for periods (left) and amplitudes(right) for the light curve of F125W and F160W. The bin size for histograms of period is 0.25 hour and for that of amplitude is 0.5%. Histograms are normalized in the way that total area of the histogram equals to 1. In the right panel, Gaussian profiles are fitted to the histograms and plotted in solid lines.

- time variability for 2M1207 B was discovered, the light curve of 2M1207 B for both two colors can be fitted with a T=10.7 hr sinusoidal curve.
- constrain on the amplitude of the amplitude of the variability. Large amplitude can be excluded. Constraints on the inhomogeniety of the cloud coverage can be inferred – small thickness variance...
- ? The atmosphere and cloud structure of 2M1207 B. How does it compare to the brown dwarf.

REFERENCES

Berta, Z. K., Charbonneau, D., Désert, J.-M., et al. 2012, ApJ, 747, 35

Biretta, J. 2014, Space Telescope WFC Instrument Science Report, 1, 10

Bonnefoy, M., Chauvin, G., Lagrange, A.-M., Rojo, P., Allard, F., Pinte, C., Dumas, C., & Homeier, D. 2014, A&A, 562, A127
Dressel, L. 2012, Wide Field Camera 3, HST Instrument Handbook, 1
Kreidberg, L., Bean, J. L., Désert, J.-M., et al. 2014, Nature, 505, 69
Mandell, A. M., Haynes, K., Sinukoff, E., et al. 2013, ApJ, 779, 128
Mohanty, S., Jayawardhana, R., Huelamo, N., & Mamajek, E. 2007, ApJ, 657, 1064
Patience, J., King, R. R., De Rosa, R. J., & Marois, C. 2010, A&A, 517, A76
Song, I., Schneider, G., Zuckerman, B., Farihi, J., Becklin, E. E., Bessell, M. S., Lowrance, P., & Macintosh, B. A. 2006, ApJ, 652, 724